Nanoscale

ROYAL SOCIETY OF CHEMISTRY

COMMUNICATION

View Article Online
View Journal | View Issue



Cite this: *Nanoscale*, 2021, **13**, 1596

Received 29th September 2020,
Accepted 20th December 2020

DOI: 10.1039/d0nr06995g

rsc.li/nanoscale



# A CHA-based DNA stochastic walker that traverses on cell membranes†

Yanlei Hu and Xia Chu *

**DNA walkers, imitating protein motors, are a class of nucleic acid nanodevice that can move along a precisely defined "track". With a promising future in materials and biotechnology, DNA walkers have gained extensive attention among researchers. Here, we introduce a catalytic hairpin assembly (CHA)-based DNA walker on cell membranes. We designed hairpin strand (H1) modified cells as tracks. Driven by DNA strand exchange, catalytic strands move on cell membranes and other hairpin strands (H2) in the solution are loaded on cells. Additionally, we also introduce a CHA-based DNA motor and use the motor for cell membrane target sensing.**

The specificity and predictability of Watson–Crick base pairing make DNA a powerful material for engineering at the nanoscale. Programmable hybridization of complementary strands has created versatile DNA static/dynamic structures, like DNA circuits, nanostructures and nanodevices.[1] Diverse DNA dynamic structures, including DNA logic gates and DNA walkers, have been designed through DNA strand exchange.[2–4]

DNA walkers, imitating protein motors, were developed around 2004.[5–9] The walkers were propelled by adding fuel strands or breaking DNA or RNA strands with an enzyme, and can move along DNA tracks autonomously. In recent years, DNA walkers not only extended the dimensions of the track, but also progressed in its function. With the development of DNA origami, researchers performed DNA walkers on a two-dimensional origami platform, which were called molecular robots or DNA motors. Choi's group designed a DNAzyme-based walker, which was synthesized by attaching DNAzyme to quantum dots and decorating RNA on carbon nanotubes.[10,11] Powered by cleaving RNA with DNAzyme, the DNA walker can controllably transport a quantum dot along the carbon nanotube. Salaita's group developed a DNA-based motor, which was composed of a DNA-coated spherical particle and an RNA-modified gold substrate.[12] When the motor was powered by hydrolyzing RNA strands with RNase H, it could move on the two-dimensional substrate in a stochastic manner. Yan's group designed a DNAzyme-based molecular walker on DNA origami.[13] The DNAzyme-conjugated streptavidin molecule extracted chemical energy from its substrate molecules and realized directional movement on a precisely defined origami.

In 2015, Ellington's group developed a stochastic DNA walker on a microparticle surface, which was based on catalytic hairpin assembly (CHA).[14] Hairpin strands (H1) anchored on microparticles interacted with catalytic strands by toehold-mediated strand exchange, hybridized with other hairpin strands (H2) and released the catalytic strands for the next cycle. As strand exchange proceeded, catalytic strands could randomly move on the microparticle surfaces, and H2 strands in the solution were loaded on the microparticle surfaces. In 2017, an autonomous DNA walker that performed on live cell membranes was developed by Tan's and You's groups cooperatively.[15,16] They anchored quencher-labelled DNA strands on cell membranes directly and dye-labelled DNA strands indirectly. After adding initiator strands, dye-labelled strands hybridized with quencher-labelled strands through toehold-mediated DNA strand exchange and realized autonomous walk. The walker was successfully applied to study encounter events on membrane domains.

Plasma membranes play an important role in cellular communication. A DNA walker on a plasma membrane provides a useful strategy for modifying living cells, simulating cell behaviour, manipulating cell functions, identifying cell types and for sensing applications.[17–19] Recently, our group and others have developed DNA walkers and used them for analytical and diagnostic applications, like nucleic acid detection, protein sensing and cancer therapy.[20–30] However, DNA walkers that perform on cell membranes are rarely reported and their study remains limited. Inspired by Ellington's work, we wondered whether a CHA-based DNA walker could perform on cell membranes. In CHA, two hairpins are kinetically trapped. By

*State Key Laboratory of Chemo/Bio-Sensing and Chemometrics, College of Chemistry and Chemical Engineering, Hunan University, Changsha 410082, P. R. China. E-mail: xiachu@hnu.edu.cn*

†Electronic supplementary information (ESI) available: Experimental section and supplementary figures. See DOI: 10.1039/d0nr06995g

adding catalytic strands, the hairpins lead to the formation of a double-stranded nucleic acid *via* toehold-mediated strand exchange.[31,32] The signal amplification method may provide an effective method for biological applications of a DNA walker on cell membranes.

For a CHA-based DNA walker on cell membranes, cells will uptake DNA probes and dead cells will release DNase into solution, which will degrade the DNA probes.[15,33] Besides that, the temperature impacts the stability of the complex between DNA amphiphiles and cell membranes.[17] As we know, endocytosis and enzyme activity can be inhibited at 4 °C.[34] However, low temperature confines the association and dissociation rate of catalysts to H1 strands, and limits the toehold-mediated CHA reaction. The influences of these factors for a CHA-based DNA walker on cell membranes were still elusive. So, it remains challenging and necessary to construct a CHA-based DNA walker that traverses on cell membranes.

We designed CHA on cell membranes with single- or double-catalyst strands (Fig. 1). For a single-catalyst (Fig. 1a), the catalyst strand hybridizes with the toehold of the cell-membrane-anchored H1 and unfolds the hairpin *via* toehold-mediated branch migration. A newly exposed region of H1 then hybridizes with the toehold of H2 and triggers strand exchange, forming a tripartite complex of H1, H2 and the single-catalyst. As strand displacement goes on, the complex resolves into a more thermodynamically stable duplex (H1 : H2) and releases the single-catalyst, which can then participate in the next recycling. For the double-catalyst (Fig. 1b), the catalyst strand contains two catalyst domains connected by a 41 bp spacer and would catalyse the adjacent hairpin assembly reaction. The double-catalyst may persist for a longer period of time and realize walking on cell membranes.

We first tested the CHA reaction in 1× PBS/$MgCl_2$ (containing 5 mM $MgCl_2$ in 1× PBS). The CHA reaction was carried out at 4 °C, 15 °C (about 5 °C lower than the melting temperature of the toehold) and 37 °C. The gel electrophoresis analysis is displayed in Fig. S1.† As can be seen, the CHA product increased and the reactant (H1 and H2) reduced with an increase in temperature. It is worth noting that the CHA reaction could also be performed efficiently at 15 °C in 1× PBS/$MgCl_2$.

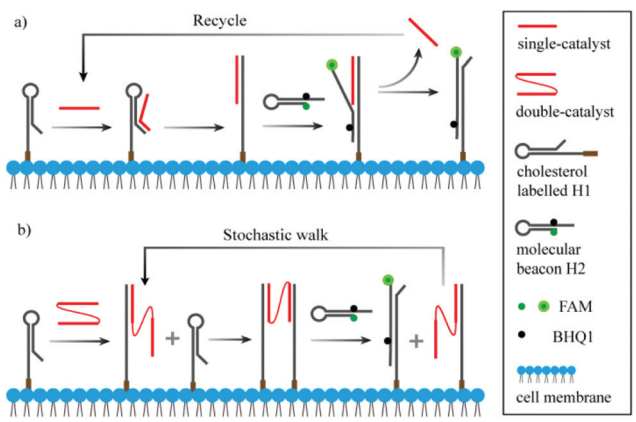


**Fig. 1** Schematic illustrations of CHA on cell membranes. (a) A schematic diagram of CHA with a single-catalyst, illustrating how the quenched molecular beacon H2 is catalytically hybridized to the membrane-anchored H1 and fluoresces. (b) A schematic diagram of CHA with a double-catalyst, illustrating how the walking behaviour is realized.

We also investigated the incubation time for anchoring H1 strands on cell membranes. H1 strands were modified with cholesterol at the 3′ end and with FAM at the 5′ end. Cells were incubated with 250 nM H1 strands at 4 °C in working buffer (containing 5 mM $MgCl_2$, 4.5 g $L^{-1}$ glucose and 1 mg $mL^{-1}$ bovine serum albumin in 1× PBS). The fluorescence of the cells was measured with flow cytometry at different time points. As displayed in Fig. S2,† the fluorescence intensity increased in the first 30 min and declined slowly from 30 min to 90 min. So, we selected 30 min for anchoring H1 strands on cell membranes.

We then tested CHA on cell membranes with a single-catalyst (Fig. 1a). As low temperature restricts endocytosis, DNase activity and the CHA reaction, we performed CHA on cell membranes with a single-catalyst at 4 °C, 15 °C and 37 °C. The results were different from those of the CHA reaction in solution (Fig. S3†). The fluorescence intensity at 15 °C was higher than those at 4 °C or 37 °C. This may be related to enzyme activity, endocytosis and the equilibrium of anchoring DNA between the working buffer and the cell surface, which are greatly influenced by temperature. Then we performed CHA on cell membranes with a single-catalyst at 15 °C. As displayed in Fig. 2a and b, the fluorescence intensity increased quickly in the first 30 min and changed slightly in the next 30 min. Considering cell death, we selected 30 min for the next experiments.

To demonstrate the recycling of catalyst strands, we designed two control experiments: a no-catalyst control (without a catalyst but with molecular beacon H2) and a non-catalyst control (with an FAM-labelled catalyst but without molecular beacon H2). We performed CHA on cell membranes with no-catalyst, non-catalyst and a 10 nM single-catalyst. As shown in Fig. 2b, no obvious fluorescence changes could be observed in 60 min for no-catalyst control or non-catalyst control experiments. However, the fluorescence with a 10 nM single-catalyst increased quickly and achieved approximately 4 times the fluorescence intensity of the non-catalyst control at 60 min. These results demonstrated that the single-catalyst indeed realized recycling for catalyzing CHA on cell membranes.

To confirm the prediction that CHA would be performed on cell membranes, we carried out CHA on cells membranes with a single-catalyst and imaged the cells with confocal microscopy. Cell images showed a ring in the FAM channel, and the ring colocalized perfectly with the cell edge in the DIC channel (Fig. S7 and S8†). These results show that CHA occurred on the cell membranes, indicating that the CHA can occur on cell membranes.

We also investigated CHA on cell membranes with a double-catalyst. As expected, fluorescence intensity at 15 °C was higher than those at 4 °C or 37 °C (Fig. S3†). The fluorescence intensity increased quickly in the first 30 min and

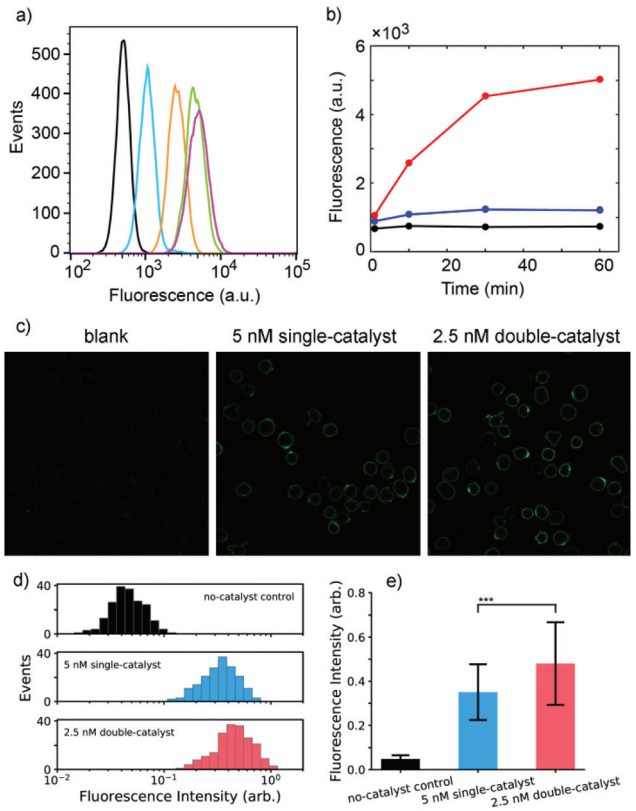


**Fig. 2** (a) Flow cytometry data of CHA on cell membranes with 10 nM single-catalyst at different time points (black line: CEM cells, light blue line: 1 min, orange line: 10 min, green line: 30 min, pink line: 60 min). (b) Fluorescence intensity changes of CHA on cell membranes *vs.* reaction time (black line: no-catalyst control (without catalyst but with H2), blue line: non-catalytic control (with FAM-labelled catalyst but without H2), red line: 10 nM single-catalyst). (c) Images of CHA on cell membranes with single-catalyst and double-catalyst. (d) Analysis of cell fluorescence intensities measured from images ($n$ = 180–200 cells from 3 biological replicates, black column: no-catalyst control, blue column: 5 nM single-catalyst, red column: 2.5 nM double-catalyst). (e) Cell fluorescence intensities measured from images (mean ± SD, $n$ = 180–200 cells from 3 biological replicates, black column: no-catalyst control, blue column: 5 nM single-catalyst, red column: 2.5 nM double-catalyst, ***$P$ < 0.01 $t$-test).

changed slightly in the next 30 min (Fig. S5†). The cell images showed a ring in the FAM channel, which colocalized with the cell edge in the DIC channel (Fig. S7†).

To verify the prediction that the double-catalyst walks on cell membranes, we prepared two different types of probes to be anchored on cell membranes: H1 and catalyst-hybridized H1 (Fig. S6a†). About 1% of H1 strands were pre-hybridized with catalyst. H1 and catalyst-hybridized H1 were anchored on cell membranes separately. Catalyst-primed and catalyst-unprimed cells were mixed in a 50% : 50% ratio and incubated with molecular beacon H2 for 30 min. Then fluorescence intensity was measured with flow cytometry. If the double-catalyst walked on the cell membranes, catalyst-primed cells should be turned on, whereas catalyst-unprimed cells should not be turned on. As shown in Fig. S6b,† the fluorescence of the cells displayed a bimodal distribution, implying that the double-catalyst strands could stand on the primed cells and realize stochastic walk.

We then compared CHA on cell membranes catalyzed by a single-catalyst with that catalyzed by a double-catalyst. With equal catalytic domains, the fluorescence intensity catalyzed by the double-catalyst was significantly higher than that catalyzed by the single-catalyst (Fig. 2d, e and Fig. S9†), indicating that the double-catalyst persisted on the cell membranes for a longer period of time and improved catalytic efficiency.

To further investigate CHA on cell membranes, we designed another type of DNA walker (Fig. 3a). Strictly speaking, it is a CHA-based DNA motor on cell membranes. An anchoring-catalyst and cholesterol-labelled H1 were anchored on the cell membranes successively. The catalyst strands opened nearby anchored H1 and promoted the hybridization of H1 and H2. The result was similar to CHA on cell membranes with a single-catalyst or a double-catalyst (Fig. S10, S11 and S12†). The fluorescence signal increased quickly in the first 30 min and changed slightly in the next 30 min. Cell images gave a ring in the FAM channel, which colocalized with the cell edge in the DIC channel. The fluorescence intensity with 20 nM of anchoring-catalyst was nearly twice that with 10 nM of anchoring-catalyst (Fig. S13†).

We then applied the CHA-based DNA motor to recognize cell membrane targets (Fig. S14a†). We designed a TC01-catalyst probe, which connected a TC01 aptamer to a catalyst strand with a 20 bp spacer. The target of the TC01 aptamer is unknown and it shows high expression in Ramos, CEM and Toledo cells.[15,35] We preformed the CHA-based DNA motor on cell membranes with a TC01-catalyst, and measured the fluorescence with flow cytometry. The cell fluorescence intensity with a TC01-catalyst was more than twice that with a non-aptamer-catalyst (Fig. S14b†).

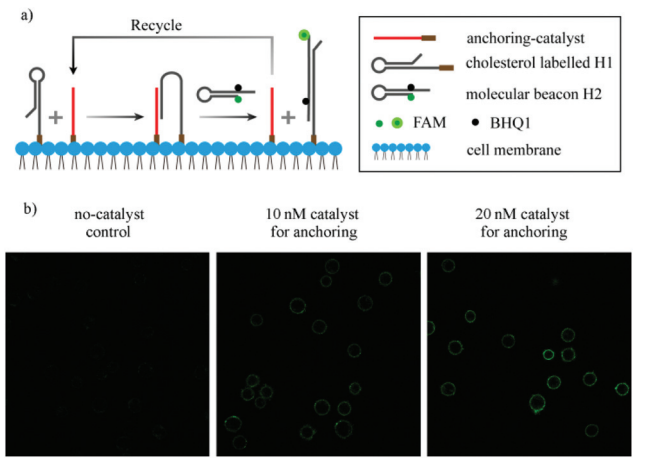


**Fig. 3** (a) A schematic illustration of CHA with an anchoring-catalyst illustrating how the motor works. (b) Images of CHA on cell membranes with an anchoring-catalyst.

## Conclusions

In conclusion, we developed a CHA-based stochastic DNA walker and demonstrated that the walker traverses on cell membranes *via* flow cytometry data and confocal images. We investigated the performance of CHA on cell membranes with a single-catalyst, a double-catalyst, and an anchoring-catalyst, and found that temperature is important for CHA on cell membranes. Additionally, we also designed a CHA-based DNA motor and used the motor for recognizing cell membrane targets. Therefore, our research is likely to promote studies of DNA walkers on cell membranes, and this can be applied to recognize membrane targets, manipulate cell functions, and actuate cells.

## Conflicts of interest

There are no conflicts to declare.

## Acknowledgements

This work was supported by the National Natural Science Foundation of China (no. 21991080 and 21525522), the Foundation for Innovative Research Groups of NSFC (grant 21521063), Hunan Provincial Science and Technology Department (no. 2019RS3011), and the Fundamental Research Funds for the Central University.

## References

1 D. Y. Zhang and G. Seelig, *Nat. Chem.*, 2011, **3**, 103–113.
2 M. von Delius and D. A. Leigh, *Chem. Soc. Rev.*, 2011, **40**, 3656–3676.
3 T. R. Kelly, *Angew. Chem., Int. Ed.*, 2005, **44**, 4124–4127.
4 Y. Li, X. C. Teng, K. X. Zhang, R. J. Deng and J. H. Li, *Anal. Chem.*, 2019, **91**, 3989–3996.
5 J. H. Reif, *Natl. Comput.*, 2003, **2**, 439–461.
6 J. S. Shin and N. A. Piercsse, *J. Am. Chem. Soc.*, 2004, **126**, 10834–10835.
7 P. Yin, H. Yan, X. G. Daniell, A. J. Turberfield and J. H. Reif, *Angew. Chem., Int. Ed.*, 2004, **43**, 4906–4911.
8 J. Bath, S. J. Green and A. J. Turberfield, *Angew. Chem., Int. Ed.*, 2005, **44**, 4358–4361.
9 Y. Tian, Y. He, Y. Chen, P. Yin and C. D. Mao, *Angew. Chem., Int. Ed.*, 2005, **44**, 4355–4358.
10 T. G. Cha, J. Pan, H. R. Chen, J. Salgado, X. Li, C. D. Mao and J. H. Choi, *Nat. Nanotechnol.*, 2014, **9**, 39–43.
11 T. G. Cha, J. Pan, H. R. Chen, H. N. Robinson, X. Li, C. D. Mao and J. H. Choi, *J. Am. Chem. Soc.*, 2015, **137**, 9429–9437.
12 K. Yehl, A. Mugler, S. Vivek, Y. Liu, Y. Zhang, M. Z. Fan, E. R. Weeks and K. Salaita, *Nat. Nanotechnol.*, 2016, **11**, 184–190.
13 K. Lund, A. J. Manzo, N. Dabby, N. Michelotti, A. Johnson-Buck, J. Nangreave, S. Taylor, R. J. Pei, M. N. Stojanovic, N. G. Walter, E. Winfree and H. Yan, *Nature*, 2010, **465**, 206–210.
14 C. Jung, P. B. Allen and A. D. Ellington, *Nat. Nanotechnol.*, 2016, **11**, 157–163.
15 M. X. You, Y. F. Lyu, D. Han, L. P. Qiu, Q. L. Liu, T. Chen, C. S. Wu, L. Peng, L. Q. Zhang, G. Bao and W. H. Tan, *Nat. Nanotechnol.*, 2017, **12**, 453–459.
16 J. Wang and Q. Yuan, *Sci. China: Chem.*, 2017, **60**, 687–688.
17 S. D. Huo, H. Y. Li, A. J. Boersma and A. Herrmann, *Adv. Sci.*, 2019, **6**, 17.
18 M. Schade, A. Knoll, A. Vogel, O. Seitz, J. Liebscher, D. Huster, A. Herrmann and A. Arbuzova, *J. Am. Chem. Soc.*, 2012, **134**, 20490–20497.
19 K. X. Zhang, H. Gao, R. J. Deng and J. H. Li, *Angew. Chem., Int. Ed.*, 2019, **58**, 4790–4799.
20 J. Liu, *Trends Anal. Chem.*, 2020, **124**, 115818.
21 W. Wang, S. Yu, S. Huang, S. Bi, H. Han, J. R. Zhang, Y. Lu and J. J. Zhu, *Chem. Soc. Rev.*, 2019, **48**, 4892–4920.
22 Y. K. Xing, B. Liu, J. Chao and L. H. Wang, *RSC Adv.*, 2017, **7**, 47425–47434.
23 J. Chen, Z. Luo, C. Sun, Z. Huang and Y. Li, *Trends Anal. Chem.*, 2019, **120**, 115626.
24 S. G. Harroun, C. Prévost-Tremblay, D. Lauzon, A. Desrosiers, X. Wang, L. Pedro and A. Vallée-Bélisle, *Nanoscale*, 2018, **10**, 4607–4641.
25 L. D. Wang, R. J. Deng and J. H. Li, *Chem. Sci.*, 2015, **6**, 6777–6782.
26 C. Liu, Y. L. Hu, Q. S. Pan, J. T. Yi, J. Zhang, M. M. He, M. Y. He, T. T. Chen and X. Chu, *Biosens. Bioelectron.*, 2019, **136**, 31–37.
27 A. Chen, Y. Zhuo, Y. Chai and R. Yuan, *Chem. Commun.*, 2019, **55**, 13932–13935.
28 Y. Wang, N. Hu, C. Liu, C. Nie, M. He, J. Zhang, Q. Yu, C. Zhao, T. Chen and X. Chu, *Nanoscale*, 2020, **12**, 1673–1679.
29 X. Chao, H. Yuqing, D. Junduan, Z. Lin, W. Huimeng, L. Yuhong, L. Juan, L. Chun-Hua and Y. Huang-Hao, *ACS Appl. Mater. Interfaces*, 2018, **10**, 32579–32587.
30 H. Gao, K. X. Zhang, X. C. Teng and J. H. Li, *Trends Anal. Chem.*, 2019, **121**, 13.
31 B. L. Li, A. D. Ellington and X. Chen, *Nucleic Acids Res.*, 2011, **39**, 13.
32 Z. Z. Jiang, H. Wang, X. B. Zhang, C. H. Liu and Z. P. Li, *Anal. Methods*, 2014, **6**, 9477–9482.
33 B. Heng, C. Cowan and S. Basu, *Cytotechnology*, 2008, **58**, 69–75.
34 H. Y. Liu and A. P. R. Johnston, *Angew. Chem., Int. Ed.*, 2013, **52**, 5744–5748.
35 Z. Tang, D. Shangguan, K. Wang, H. Shi, K. Sefah, P. Mallikratchy, H. W. Chen, Y. Li and W. Tan, *Anal. Chem.*, 2007, **79**, 4900–4907.